Combustion and Flame 204 (2019) 380–390

Contents lists available at ScienceDirect

Combustion and Flame

journal homepage: www.elsevier.com/locate/combustflame

Ignition delay times of ethane under O_2/CO_2 atmosphere at different pressures by shock tube and simulation methods

Yang Liu, Jia Cheng, Chun Zou*, Lixin Lu, Huixiang Jing

State Key Laboratory of Coal Combustion, Huazhong University of Science and Technology, Wuhan 430074, PR China

ARTICLE INFO

Article history:
Received 18 December 2018
Revised 24 January 2019
Accepted 22 March 2019
Available online 1 April 2019

Keywords:
Ethane
O_2/CO_2 atmosphere
Ignition delay time
Optimized model
Model evaluation

ABSTRACT

Pressurized oxy-fuel combustion is a promising oxy-fuel technology owing to its high efficiency and low emission. The ignition delay times of ethane under O_2/CO_2 atmosphere were determined in a shock tube at different pressures, equivalence ratios, and C_2H_6 and CO_2 concentrations. The results suggested that the ignition delay times decrease with the increasing ethane concentration at 0.8, 2.0, and 10 bar, while the effect of the fuel concentration on the ignition delay times is not sensitive to the pressure. The ignition delay times increased with the increasing equivalence ratio at 0.8 and 2.0 bar, while the effect of the equivalence ratio decreased with the increasing pressure from 0.8 to 2.0 bar. At 10 bar, the effect of the equivalence ratio on the ignition delay times further weakened at high temperatures, while the ignition delay times decreased with the increasing equivalence ratio in the low-temperature range. An updated model (OXYMECH) was developed and updated on the basis of our previous work, providing yields in good agreement with the experimental data under all conditions, while Aramco 2.0 showed poor prediction of the experimental results at 10 bar. Analysis of the sensitivity and the rate of production indicated that updating the rate constants of the reactions $C_2H_6 + HO_2 \Leftrightarrow C_2H_5 + H_2O_2$, $H + O_2 (+M) \Leftrightarrow HO_2 (+M)$, $CH_3 + HO_2 \Leftrightarrow CH_3O + OH$, $2HO_2 \Leftrightarrow H_2O_2 + O_2$, $C_2H_4 + H (+M) \Leftrightarrow C_2H_5 (+M)$, and $H + O_2 \Leftrightarrow O + OH$ improves the performance at 10 bar.

1. Introduction

Pressurized oxy-fuel combustion is regarded as a new generation of oxy-fuel technology owing to its high efficiency and low emission [1], which has recently been attracting increasing attention among researchers [2–4]. As fundamental components of pressurized oxy-fuel combustion, the ignition and combustion kinetics of the fuel under O_2/CO_2 atmosphere and high pressure have been studied by many researchers [5–10].

Shock tubes are typically used to measure the ignition delay time of fuels, which is a key parameter to develop and validate chemical kinetic models for fuels. Ethane is an important component in natural and shale gas and a critical intermediate in the oxidation and pyrolysis of hydrocarbon fuels and coal [11–14]. The ignition delay times and chemical kinetic models of ethane diluted in Ar have been studied by many researchers [15–19]. Pan et al. [15] investigated the ignition delay times of $C_2H_6/H_2/O_2/Ar$ mixtures at elevated pressures using a shock tube. They found that Aramco 1.3 [20] results showed good agreement with the measurements for all mixtures. Hu et al. [16] studied experimentally and numerically the ignition delay times of ethane with the diluent argon at different equivalence ratios ($\Phi = 0.5$, 1.0, and 2.0) and pressures ($P = 1.2$, 5, and 20 atm). They reported that Aramco 1.3 well predicted the experimental data compared to GRI 3.0 [21]. Zhang et al. [17] performed a study of ethane ignition with Ar dilution at 1.2 and 5.3 atm under stoichiometric conditions, in which they observed that the predictions of NUIG C4 [22] were better than those of USC 2.0 [23]. It is obvious that Aramco 1.3 and NUIG C4 satisfactorily predict the ignition delay times of ethane under O_2/Ar atmosphere. However, experimental data and model validation of the ignition delay times of ethane under O_2/CO_2 atmosphere have not been realized to date.

Some studies have focused on the performance of models in pressurized oxy-fuel through the ignition delay times of methane and syngas in shock tubes [24–26]. Liu et al. [24] evaluated the performance of FFCM-1 [27], Aramco 1.3, "Ranzi" [28], USC 2.0, and GRI 3.0 models using the ignition delay times of methane under O_2/CO_2 atmosphere at pressures of 0.8, 1.75, and 10 atm, and found that none of the models fitted suitably the experimental data, where Aramco 1.3 in particular overpredicted the experimental data at 0.8 and 1.75 atm. Barak et al. [5,25] studied the ignition delay times of syngas under O_2/CO_2 atmosphere in the pressure

* Corresponding author.
E-mail address: zouchun@hust.edu.cn (C. Zou).

https://doi.org/10.1016/j.combustflame.2019.03.031
0010-2180/

ranges of 1.61–1.77 and 34.58–45.50 atm and evaluated the performance of different kinetic models; they noticed that Aramco 2.0 [29] was inaccurate in predicting experimental results at both low and high pressures. CO_2 is not chemically inert; indeed, it can participate in certain chemical reactions. It was, thus, obvious that models such as Aramco 2.0, "Ranzi", USC 2.0, and GRI 3.0 do not satisfactorily predict the ignition delay times of methane and syngas under O_2/CO_2 atmosphere at both low and high pressures.

Moreover, the reaction rate of the third-body reaction can be enhanced under O_2/CO_2 atmosphere because of the chaperon effect of CO_2. Many researchers [15–17,19] have suggested that the third-body reaction $C_2H_4 + H\ (+M) \Leftrightarrow C_2H_5\ (+M)$ is very important for ethane ignition delay times. Lee et al. [30] studied the ignition delay times in $H_2/CO/CO_2$ mixtures. They modified the reaction rate constant of $H + O_2\ (+CO_2) \Leftrightarrow HO_2\ (+CO_2)$ in Aramco 1.3 to reconcile the discrepancies between the simulated and measured results at pressures of 1.24–2.36 atm and temperatures below 1025 K. With the development of shock tube methods and multi-species laser absorption diagnostics [31], more accurate reaction rate constants can be determined in shock tubes. Shao et al. [32] determined the reaction rate constants of $H + O_2 + M \Leftrightarrow HO_2 + M$ (M = Ar, N_2, CO_2, H_2O) through ignition delay time measurements in a shock tube. Wang et al. [33] determined the rate constant of $OH + CO \Leftrightarrow CO_2 + H$ by laser absorption measurements of OH and CO in a shock tube. Thus, a model updated by the findings in these studies can suitably predict the ignition delay times of ethane under O_2/CO_2 atmosphere.

In this study, the ignition delay times of ethane under O_2/CO_2 atmosphere were measured in a shock tube at pressures of 0.8, 2.0, and 10 bar, equivalence ratios of 0.5, 1.0, and 2.0, and in the temperature range of 1064–1550 K. The effects of fuel concentration, equivalence ratio, and CO_2 concentration on the ignition delay times of ethane were evaluated using the experimental results. A modified model, named OXYMECH, is proposed based on our previous model [24]. Three detailed chemical kinetic models (Aramco 2.0, "Ranzi", and OXYMECH) were compared using the present experimental data. Finally, a detailed comparison of Aramco 2.0 and OXYMECH was carried out at a pressure of 10 bar.

2. Experimental methods

The experimental results in this study were measured in a shock tube with an inner diameter of 10 cm. The experimental method has been reported in detail in our previous work [24], and only a brief description is provided in the present study. The shock tube contains an 8 m driven section and a 4 m driver section. At 0.8 and 2.0 bar, the two sections are separated by a polyester terephthalate (PET) diaphragm, which is burst by a built-in spring needle to produce a shock wave. At 10 bar, the two sections are separated by two PET diaphragms, which are burst by sudden venting of the gas between the two diaphragms to create a shock wave. The thickness of the diaphragms was 50, 75, and 125 μm at 0.8, 2.0, and 10 bar, respectively. High-pressure air was used to clean the shock tube before all the experiments. The mixing tank and the shock tube were evacuated to $<1 \times 10^{-6}$ bar with two oil-sealed, sliding, vane rotary vacuum pumps (Oerlikon Leybold TRIVAC D40T) and two root pumps (Oerlikon Leybold Ruvac WAU501). As show in Table 1, eight experimental mixtures were tested in this study. Dalton's law of pressure was applied while preparing the mixtures, which were allowed to settle for more than 12 h in a 300 L mixing tank. The purities of ethane, oxygen, carbon dioxide, and argon were 99.99%, 99.999%, 99.999%, and 99.999%, respectively.

The incident shock velocity was obtained using five piezoelectric pressure transducers (PCB 111A24) placed alongside the tube at intervals of 20 cm. The pressure time history was monitored through a piezoelectric pressure transducer (Kistler 603B1) placed

Table 1
Composition of the experimental mixtures and conditions.

Mixture	Φ	C_2H_6	O_2	CO_2	Ar	Pressure (bar)
mix-1	0.5	0.02	0.14	0	0.84	0.8,2,10
mix-2	0.5	0.02	0.14	0.3	0.54	0.8,2
mix-3	0.5	0.02	0.14	0.6	0.24	0.8,2,10
mix-4	0.5	0.02	0.14	0.84	0	0.8,2,10
mix-5	1	0.04	0.14	0.6	0.22	0.8,2,10
mix-6	1	0.02	0.07	0.6	0.31	0.8,2,10
mix-7	2	0.02	0.035	0.6	0.345	10
mix-8	2	0.08	0.14	0.6	0.18	0.8,2,10

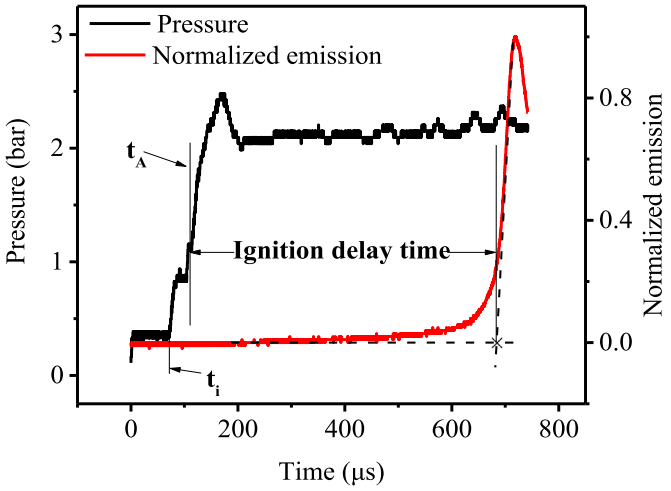

Fig. 1. Definition of ignition delay time for mix-6 at $T = 1265$ K and $P = 2.08$ bar.

0.2 cm from the end wall. A photomultiplier was installed 0.2 cm from the end wall with a band-pass filter of 307 ± 10 nm to evaluate the OH* radical emission. The Gaseq [34] program was used to calculate the temperatures and pressures behind the reflected shock. The uncertainty in the temperature was estimated as ± 23 K, and the uncertainty in the ignition delay times was estimated as 20% according to our previous study [24]. The detailed analysis of the uncertainty is provided in Supplementary Material.

As shown in Fig. 1, the ignition delay times were determined as the time interval between the onset of ignition and the arrival of the reflected wave. In this study, the onset of ignition was determined by positioning the sharpest increase in normalized OH* radical emission and linearly extrapolating to the zero baseline. An empirical expression proposed by Petersen and Hanson [35] in 2005 was used to determine the arrival of the reflected shock wave:

$$\Delta t_{AO}(\mu s) = 4.6 M_S^{0.66} \gamma_2^{-7.1} \overline{M}^{0.57} \quad (1)$$

where Ms denotes the Mach number of incident shock, γ_2 denotes the specific heat of the upstream mixture, $\overline{M}$ denotes the molecular weight of the mixture in the driven section, and t_A denotes the arrival time of the reflected shock wave, which can be defined as:

$$t_A = \Delta t_{AO} + \frac{D}{2V_R} + t_i \quad (2)$$

where D denotes the diameter of the piezoelectric pressure transducer (Kistler 603B1), V_R denotes the velocity of the reflected shock wave, and t_i denotes the time of the initial pressure rise.

3. Modeling

In our previous work, we updated a modified mechanism on the basis of Aramco 1.3, which showed good agreement with the experimental data for the ignition delay time of methane under

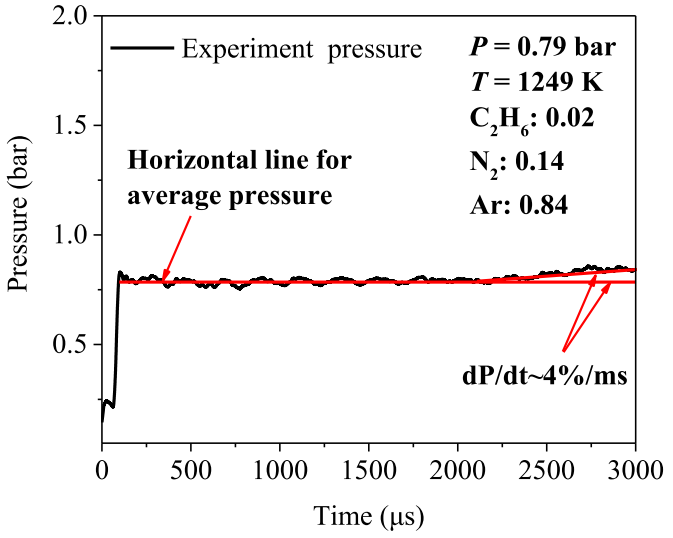

Fig. 2. Determination of non-ideal effects in the present system.

O_2/N_2 and O_2/CO_2 atmospheres [10,24]. In present study, a new modified mechanism, named OXYMECH, is proposed based on our previous work [24]. Important updated reactions result from recent advances in both experimental techniques and theoretical tools. It is important to note that reaction rate constants of these reaction have been optimized in FFCM-1 developed by the research collaboration between Hai Wang's research group at Stanford University and Gregory Smith of the SRI International. They used the Method of Uncertainty Minimization using Polynomial Chaos Expansions (MUM-PCE) [36–38] to constrain key reaction rate coefficient uncertainties and to quantify the remaining model uncertainty. Therefore, the optimized reaction rate constants of these reactions for FFCM-1 were used for OXYMECH and are listed in Table 2 in detail.

The Senkin [57] code from the CHEMKIN-II [58] package was adopted for the sensitivity analysis, and CHEMKIN-PRO was adopted for the rate of production (ROP) and conversion rate of species (CR) analyses. As shown in Fig. 2, a pressure rise (about 4%/ms) owing to non-ideal effects appeared from 2000 μs behind the reflected shock wave. Therefore, a modified ($dp/dt = 4\%/ms$) constant volume, the zero-dimensional chemistry model (U and V assumption), was adopted for ignition delay times longer than 2000 μs. Aramco 2.0, "Ranzi", and OXYMECH models were then adopted to calculate the ignition delay times.

4. Results and discussion

4.1. Facilities and method validation

In order to validate the present system and method for ethane ignition delay time measurement, the ignition delay times were determined under conditions of 2% C_2H_6, 7% O_2, and 91% Ar at 2 atm and of 5% CH_4, 20% O_2, and 75% CO_2 at 1.75 atm. Figure 3(a) shows a comparison of the ignition delay times obtained in the present study and those reported by de Vries et al. [18] for ethane under conditions of $P = 2$ atm, $\Phi = 1$, and 91% Ar dilution. It is clear that the present experimental results are in perfect agreement with those by de Vries et al. [18]. Figure 3(b) shows a comparison of the ignition delay times determined in the present study and those reported by Hargis and Petersen [10] for methane under conditions of $P = 1.75$ atm, $\Phi = 0.5$, and 75% CO_2 dilution. It can be seen that the agreement between those two studies is also very good. Therefore, the present method and system are reliable

Table 2
Important reactions optimized in the present work[a].

Number	Reaction	A	n	E_A	Source
2800	$C_2H_6 + HO_2 \Leftrightarrow C_2H_5 + H_2O_2$	1.10E + 05	2.5	16,850	[39]
2794	$C_2H_6 + OH \Leftrightarrow C_2H_5 + H_2O$	9.15E + 06	2.0	994	[39]
	Optimized R2794	9.46E + 06	2.0	994	[27]
2792	$C_2H_6 + H \Leftrightarrow C_2H_5 + H_2$	1.15E + 08	1.9	7530	[40]
	Optimized R2792	1.13E + 08	1.9	7530	[27]
2797	$C_2H_6 + CH_3 \Leftrightarrow C_2H_5 + CH_4$	5.60E + 10	0.0	9420	[39]
	Duplicate				
2798	$C_2H_6 + CH_3 \Leftrightarrow C_2H_5 + CH_4$	8.43E + 14	0.0	22,260	[39]
	Optimized R2798	8.30E + 14	0.0	22,260	[27]
	Duplicate				
2793	$C_2H_6 + O \Leftrightarrow OH + C_2H_5$	1.81E + 05	2.8	5803	[39]
	Optimized R2793	1.76E + 05	2.8	5803	[27]
2788	$C_2H_5 + O_2 \Leftrightarrow HO_2 + C_2H_4$	1.41E + 07	1.1	−1975	[41]
	Optimized R2793	1.36E + 07	1.1	−1975	[27]
2773	$C_2H_4 + H\ (+M) \Leftrightarrow C_2H_5\ (+M)$	1.37E + 09	1.5	1355	[42]
	Low-pressure limit	2.90E + 39	−6.6	5769	
	$a = 1.6$, $T^3 = -9147$, $T^1 = 299$, $T^2 = 152$				
	Optimized R2773	1.23E+09	1.5	1355	[27]
	Low-pressure limit	2.03E+39	−6.6	5769	
	$a = 1.6$, $T^3 = -9147$, $T^1 = 299$, $T^2 = 152$				
2778	$C_2H_4 + OH \Leftrightarrow C_2H_3 + H_2O$	2.14E + 04	2.7	2216	[43]
	Optimized R2778	2.14E + 04	2.7	2216	[27]
2774	$C_2H_4 + H \Leftrightarrow C_2H_3 + H_2$	2.35E + 02	3.6	11,270	[39]
	Optimized R2774	2.20E + 02	3.6	11,270	[27]
2655	$2CH_3 \Leftrightarrow H + C_2H_5$	5.0E + 12	0.1	1060	[44]
	Optimized R2655	7.62E + 12	0.1	1060	[27]
2647	$CH_3 + HO_2 \Leftrightarrow OH + CH_3O$	1.04E + 13	0.0	−590	[45,46]
	Optimized R2647	8.82E + 12	0.0	−590	[27]
2646	$CH_3 + HO_2 \Leftrightarrow O_2 + CH_4$	2.02E + 05	2.7	51,751	[47,48]
	Optimized R2646	1.27E + 05	2.2	−3022	[27]
2640	$CH_3 + O \Leftrightarrow H + CH_2O$	5.39E + 13	0.0	0	[39]
	Optimized R2640	5.72E + 13	0.0	0	[27]
2585	$HCO + H \Leftrightarrow H_2 + CO$	9.03E + 13	0.0	0	[39]
	Optimized R2585	8.48E + 13	0.0	0	[27]
2581	$CO + OH \Leftrightarrow H + CO_2$	7.05E + 04	2.1	−356	[49]
	Optimized R2581	6.19E + 04	2.1	−356	[27]
	Duplicate				
2582	$CO + OH \Leftrightarrow H + CO_2$	5.76E + 12	−0.7	332	[49]
	Optimized R2582	5.0E + 12	−0.7	332	[27]
	Duplicate				
2573	$H_2O_2\ (+M) \Leftrightarrow 2OH\ (+M)$	2.0E + 12	0.9	48,750	[50]
	Low-pressure limit	2.49E + 24	−2.3	48,750	
	$a = 0.58$, $T^3 = 30$, $T^1 = 90{,}000$, $T^2 = 90{,}000$				
	Optimized R2573	2.19E + 12	0.9	48,750	[27]
	Low-pressure limit	2.49E + 24	−2.3	48,750	
	$a = 0.58$, $T^3 = 30$, $T^1 = 90{,}000$, $T^2 = 90{,}000$				
2550	$H + O_2 \Leftrightarrow O + OH$	1.04E + 14	0.0	15,310	[51]
	Optimized R2550	9.84E + 13	0.0	15,310	[27]
2571	$2HO_2 \Leftrightarrow H_2O_2 + O_2$	1.94E + 11	0.0	−1409	[52]
	Optimized R2571	1.96E + 11	0.0	−1409	[27]
	Duplicate				
2572	$2HO_2 \Leftrightarrow H_2O_2 + O_2$	1.03E + 14	0.0	11,040	[52]
	Optimized R2572	1.11E + 14	0.0	11,040	[27]
	Duplicate				
2565	$HO_2 + H \Leftrightarrow H_2 + O_2$	3.68E + 06	2.1	−1455	[53]
	Optimized R2565	2.95E + 06	2.1	−1455	[27]
2566	$HO_2 + H \Leftrightarrow 2OH$	7.08E + 13	0.0	300	[54]
	Optimized R2566	5.89E + 13	0.0	300	[27]
2567	$HO_2 + H \Leftrightarrow O + H_2O$	1.45E + 12	0.0	0	[39]
	Optimized R2567	1.63E + 12	0.0	0	[27]
2553	$OH + H_2 \Leftrightarrow H + H_2O$	2.16E + 08	1.5	3437	[55]
	Optimized R2553	2.26E + 08	1.5	3437	[27]
2564	$H + O_2\ (+M) \Leftrightarrow HO_2\ (+M)$	4.65E + 12	0.4	0	[56]
	Low-pressure limit	6.37E + 20	−1.7	525	
	$a = 0.5$, $T^3 = 30$, $T^1 = 90{,}000$, $T^2 = 90{,}000$				
	Optimized R2564	4.57E + 12	0.4	0	[27]
	Low-pressure limit	6.37E + 20	−1.7	525	
	$a = 0.5$, $T^3 = 30$, $T^1 = 90{,}000$, $T^2 = 90{,}000$				

[a] Rate constants are expressed as $k = AT^{\beta} \exp(-E_a/RT)$ with units of calories, cm^3, mole, and s.

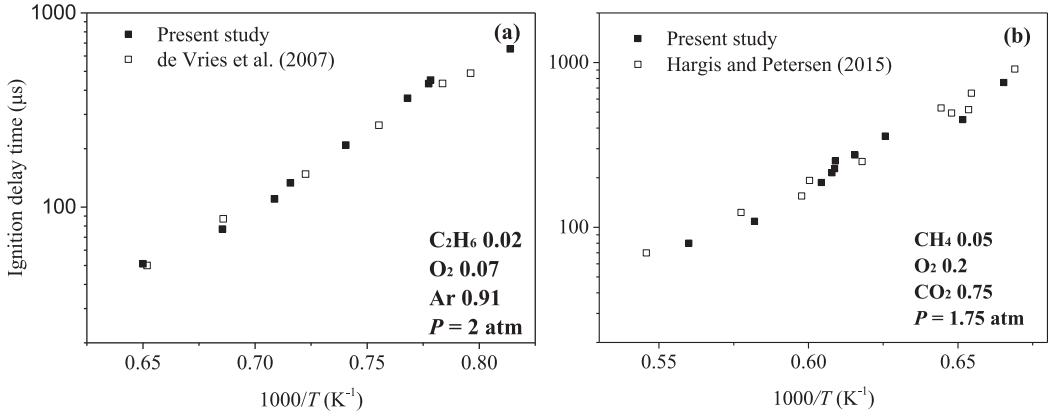

Fig. 3. Comparison of the results obtained in the present study and those reported by (a) de Vries et al. [18] and (b) Hargis and Petersen [10].

for the measurement of the ignition delay times of ethane under O_2/CO_2 atmosphere. The experimental data in this study are provided in the Supplementary Material Table S1.

4.2. Effect of the fuel concentration, equivalence ratio, and CO_2 concentration

Figure 4 shows the ignition delay times at different C_2H_6 concentrations ($XC_2H_6 = 0.02$, 0.04, and 0.08), different equivalence ratios ($\Phi = 0.5$, 1.0, and 2.0), three pressures ($P = 0.8$, 2.0, and 10 bar), and different CO_2 concentrations ($XCO_2 = 0$, 0.3, 0.6, and 0.84). As shown in Fig. 4(a), at $\Phi = 1$, the ignition delay times decrease with the increasing XC_2H_6. The differences in ignition delay times between $XC_2H_6 = 0.02$ and $XC_2H_6 = 0.04$ at 0.8, 2.0, and 10 bar are quite similar, indicating that the effect of fuel concentration on the ignition delay time of ethane under O_2/CO_2 atmosphere is not sensitive to the pressure.

As shown in Fig. 4(b) and (c), at $XO_2 = 0.14$, the ignition delay times increase with the equivalence ratio at 0.8 and 2.0 bar. A similar phenomenon for the ignition delay of ethane at 5 atm was also found by Hu et al. [16]. Moreover, the differences in the ignition delay times between $\Phi = 0.5$ and $\Phi = 1.0$ decrease with the increasing pressure from 0.8 to 2.0 bar, indicating that the effect of the equivalence ratio on the ignition delay times of ethane under O_2/CO_2 atmosphere decrease with the increasing pressure. As shown in Fig. 4(d), at 10 bar, the effect of the equivalence ratio on the ignition delay times of ethane further weakens at high temperatures; the ignition delay times at $\Phi = 0.5$, 1.0, and 2.0 are almost identical. In the low temperature range, the ignition delay times decrease with the increasing equivalence ratio. This behavior is opposite that observed at $P = 0.8$ and 2.0 bar.

As shown in Fig. 4(e) and (f), at $\Phi = 0.5$, the ignition delay times for $XCO_2 = 0$, 0.3, 0.6, and 0.84 are almost identical at 0.8 and 2.0 bar, which means that the effect of the CO_2 concentration is minimal. As shown in Fig. 4(g), at 10 bar and $\Phi = 0.5$, the ignition delay times for $XCO_2 = 0.84$ and 0.6 are longer than those for $XCO_2 = 0$, which indicates that high concentrations of CO_2 significant increase the ignition delay times of ethane. Similar phenomena have been reported for methane [10].

Both physical and chemical properties of CO_2 may impact the ignition of ethane; thus, an artificial species, X, was introduced to differentiate these two effects. X denotes a chemically inert species with the thermochemical properties of CO_2. Moreover, the percentage of ignition delay time variation (PV) [59] was introduced to study those two effects quantitatively, defined as:

$$PV_{PE} = \frac{\tau_{mix-X} - \tau_{mix-N_2}}{\tau_{mix-X}} \times 100 \quad (3)$$

$$PV_{CE} = \frac{\tau_{mix-3} - \tau_{mix-X}}{\tau_{mix-X}} \times 100 \quad (4)$$

where mix-X and mix-N_2 denote mixtures of ($C_2H_6 + X$) and ($C_2H_6 + N_2$), respectively. The mole fractions of X and N_2 are the same as that of CO_2 in mix-3. $\tau_{mix\text{-}3}$, τ_{mix-N_2}, and $\tau_{mix\text{-}X}$ denote the ignition delay times of mix-3, mix-N_2, and mix-X, respectively. PV_{PE} and PV_{CE} denote the physical and chemical effects of CO_2, respectively. As a result, the sum of PV_{PE} and PV_{CE} denotes the total effects of CO_2 ($PV_{TE} = PV_{PE} + PV_{CE}$). A positive PV indicates the suppression of ignition, while a negative PV indicates the promotion of ignition.

The ignition delay time was calculated by OXYMECH, whose validation is discussed in the next section. Figure 5 shows the percentage variation of the chemical, physical, and total effects of CO_2 on the ignition delay times of ethane in the pressure range of 0.8–10 bar. As show in Fig. 5, PV_{PE} slowly increases from 12% to 15.5% with the increasing pressure from 0.8 to 2 bar and remains unchanged at pressures of 2–10 bar, which means that the physical effect of CO_2 suppresses the ignition of ethane and is almost not sensitive to the pressure. The PV_{CE} value sharply increases from −9.3% to 17.5% with the increasing pressure from 0.8 to 8 bar, and remains constant at pressures of 8–10 bar. This means that the chemical effect of CO_2 is sharply enhanced with the increasing pressure from 0.8 to 8 bar. The profile of PV_{TE} is very similar to that of PV_{CE}, which indicates that the changes in the effects of CO_2 with the pressure are attributed to PV_{CE}. It is worth nothing that, in the low pressure range from 0.8 to 2 bar, the chemical effect promotes the ignition and is comparable to the physical effect, resulting in a low value of PV_{TE} ($PV_{TE} < 10\%$). Consequently, the ignition delay times for $XCO_2 = 0$, 0.3, 0.6, and 0.84 are almost identical at 0.8 and 2.0 bar. In the high pressure range from 7 to 10 bar, PV_{TE} is over 30%, which suggests that CO_2 significantly suppresses the ignition of ethane due to the superposition of negative chemical and physical effects. Consequently, the ignition delay times for $XCO_2 = 0.84$ and 0.6 are longer than that for $XCO_2 = 0$ at 10 bar ($PV_{TE} = 34\%$).

4.3. Model evaluation

In this study, three models, namely, OXYMECH, Aramco 2.0, and "Ranzi" were evaluated with the present ignition delay data. In the Supplementary Material, Figs. S1–S3 show a comparison of the experimental and calculated results for ethane ignition delay times under O_2/CO_2 atmosphere at pressures of 0.8, 2.0, and 10 bar and equivalence ratios of 0.5, 1.0, and 2.0. Moreover, in order to validate OXYMECH, the ignition delay times of ethane has been measured at the ethane concentration of 0.02, the N_2 concentration of 0.06, the equivalence ratio of 0.5 and three pressures ($P = 0.8$, 2.0, and 10 bar), and experimental data are shown in the Supplementary

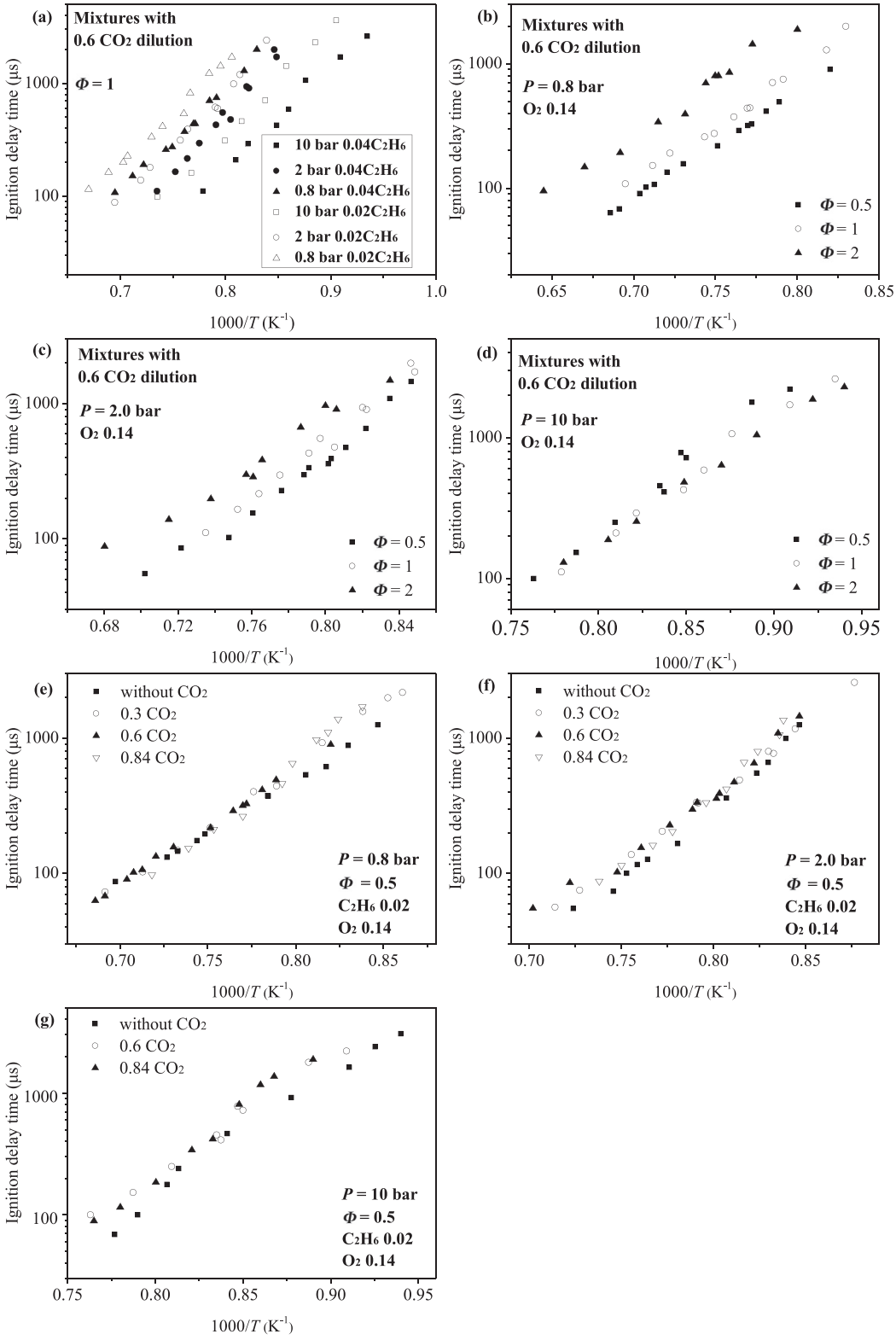

Fig. 4. Experimental results at different C_2H_6 concentrations ($XC_2H_6 = 0.02$, 0.04, and 0.08), equivalence ratios ($\Phi = 0.5$, 1.0, and 2.0), pressures ($P = 0.8$, 2.0, and 10 bar), and CO_2 concentrations ($XCO_2 = 0$, 0.3, 0.6, 0.84).

Material (Table S2). The modeling results against the ethane ignition data from OXYMECH using the ignition data for ethane under O_2/N_2 and O_2/Ar [16,18,19] are provided in the Supplementary Material (Fig. S4). It can be seen that OXYMECH affords good agreement with the experimental data for the ignition of ethane under O_2/CO_2, O_2/N_2, and O_2/Ar atmospheres at different pressures. In other words, OXYMECH was confirmed to be suitable to study the effect of CO_2 on the ignition delay times of ethane.

To quantitatively evaluate the performance of those three models for the ignition of ethane under O_2/CO_2 atmosphere, the

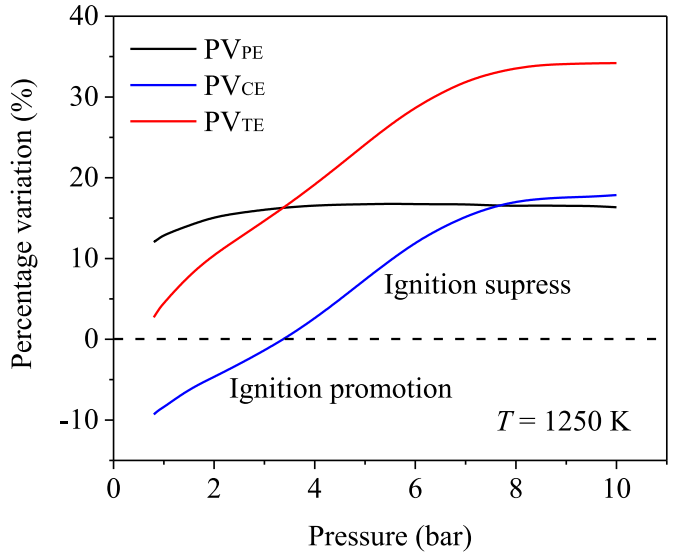

Fig. 5. Chemical, physical, and total effects of CO_2 on the ignition delay times of ethane at pressures of 0.8–10 bar.

Table 3
Average absolute relative error values for the three models and different mixtures at 0.8, 2.0, and 10.0 bar.

Pressure (bar)	Φ	XO_2	Mixture	*E* (%)		
				Aramco 2.0	"Ranzi"	OXYMECH
0.8	0.5	0.14	mix-1	7.5	46.8	7.0
0.8	0.5	0.14	mix-2	13.8	41.9	18.0
0.8	0.5	0.14	mix-3	7.5	46.8	7.0
0.8	0.5	0.14	mix-4	19.8	38.8	19.9
0.8	1	0.14	mix-5	8.9	50.5	8.5
0.8	1	0.07	mix-6	15.7	42.1	9.8
0.8	2	0.14	mix-8	19.5	62.5	14.8
2	0.5	0.14	mix-1	5.9	28.3	18.0
2	0.5	0.14	mix-2	15.2	33.2	19.7
2	0.5	0.14	mix-3	5.9	28.3	18.0
2	0.5	0.14	mix-4	7.5	8.6	16.3
2	1	0.14	mix-5	9.0	23.5	15.0
2	1	0.07	mix-6	11.5	20.4	15.3
2	2	0.14	mix-8	12.0	36.6	19.8
10	0.5	0.14	mix-1	48.2	108.9	16.5
10	0.5	0.14	mix-3	48.2	108.9	16.5
10	0.5	0.14	mix-4	47.0	93.8	18.5
10	1	0.14	mix-5	40.2	76.9	18.3
10	1	0.07	mix-6	17.2	42.8	18.6
10	2	0.035	mix-7	7.3	22.0	15.1
10	2	0.14	mix-8	19.1	40.5	19.9

average absolute error value (*E*,%) was introduced, expressed as:

$$E = \frac{1}{N}\sum_{i=1}^{N}\left|\frac{Y_{\mathrm{sim},i} - Y_{\mathrm{exp},i}}{Y_{\mathrm{exp},i}}\right| \times 100 \quad (5)$$

where N is the number of data points in the data set, and $Y_{\mathrm{sim},i}$ and $Y_{\mathrm{exp},i}$ are the calculated and measured results for the ith data point, respectively. Smaller E values indicate better performance of the model.

Table 3 lists the E values of the three models under 21 different conditions. As shown in Table 3, at 0.8 bar, the E values for OXYMECH remain below 15% in most cases, while only two conditions afford values in the range of 15–20%, which means that the OXYMECH data are in good agreement with the experimental results. At 2.0 and 10 bar, the E values are in the range of 15–20%, which indicates that the OXYMECH data still are in good agreement with the experiment results. To summarize, OXYMECH provides good fitting of the experimental data both under fuel-lean/fuel-rich and low/ high pressure conditions.

Using Aramco 2.0 at 0.8 and 2.0 bar, the E values are below 20%, which means that the Aramco 2.0 data are in good agreement with the experimental results. At 10 bar, the errors for mix-6, mix-7, and mix-8 are still below 20%, indicating that Aramco 2.0 shows good agreement with the experimental results under fuel-rich conditions and stoichiometric conditions with low oxygen concentrations. It is worth nothing that the errors for mix-1, mix-3, mix-4, and mix-5 are over 40%, suggesting that Aramco 2.0 shows poor prediction of experimental results at $P = 10$ bar, as can be seen in Fig. S3(a)–(d).

In the case of "Ranzi", there is only one condition (mix-4, $P = 2$ bar) under which the error is low (8.6%). In contrast, the E values for the other 20 conditions are over 20%. This suggests the poor prediction power of "Ranzi", except in the case of fuel-lean conditions with high CO_2 concentrations at 2.0 bar.

Moreover, the validation data for the OXYMECH model for CH_4 under O_2/N_2 and O_2/CO_2 atmosphere at three pressures (0.8, 2.0, and 10 bar) [10,24], CH_4 under O_2/Ar atmosphere [60–62], and H_2 under O_2/Ar atmosphere [62–64] are provided in the Supplementary Material (Fig. S5–S7). It is obvious that OXYMECH provides good predictions of the ignition delay times of CH_4, C_2H_6, and H_2 in various conditions.

4.4. Comparison of Aramco 2.0 with OXYMECH at P = 10 bar and T = 1050 K

Since Aramco 2.0 shows poor prediction of the experimental data at 10 bar, a sensitivity comparison was performed with Aramco 2.0 and OXYMECH for mix-3 ($XC_2H_6 = 0.02$, $XO_2 = 0.14$, $XCO_2 = 0.6$, $XAr = 0.24$) under conditions of $P = 10$ bar and $T = 1050$ and 1350 K. The sensitivity coefficients (σ) were calculated using the following formula:

$$\sigma_i = \frac{\tau(2.0k_i) - \tau(0.5k_i)}{\tau(k_i)} \quad (6)$$

where ki is the rate constant of the ith reaction, τ is the ignition delay time, and σ_i is the sensitivity coefficient of the ith reaction.

Figure 6 presents the top 12 reactions with high sensitivity coefficients for mix-3 at $P = 10$ bar and $T = 1050$ K using Aramco 2.0 and OXYMECH. For those two models, the reaction $C_2H_6 + HO_2 \Leftrightarrow C_2H_5 + H_2O_2$ (R2800) has the highest sensitivity coefficient, suggesting that R2800 is the most important reaction to promote the ignition of ethane at 10 bar under fuel-lean and low temperature conditions. Because the reaction rate constants of R2800 from Aramco 2.0 and OXYMECH were sourced from different reports [39,65], there is a 47.5% difference in the rate constant between Aramco 2.0 and OXYMECH, as shown in Fig. 7(a), which results in a different net reaction rate. Figure 8(a) shows a comparison of Aramco 2.0 and OXYMECH for the net reaction rate of R2800 at $P = 10$ bar and $T = 1050$ K. It can be seen that the increase in the net reaction rate of R2800 in OXYMECH is sharper than that in Aramco 2.0 during the initial ignition period. Moreover, from the analysis of rate of production (ROP), R2800 remains the second reaction for H_2O_2 production. Therefore, the mole fraction of H_2O_2 calculated with OXYMECH increases faster than that using Aramco 2.0, as shown in Fig. 8(b).

Obviously, HO_2 is the key species to the ignition in the low temperature ranges. HO_2 is mainly derived from the reaction $H + O_2$ (+M) $\Leftrightarrow$ HO_2 (+M) (R2564) according to ROP. For R2564, because the reaction rate constants from Aramco 2.0 and OXYMECH were sourced from different reports [56,66], the reaction rate constant of R2564 using OXYMECH is 1.29 times higher than that provided by Aramco 2.0 at 1050 K, as shown in Fig. 7(b). As a result, in OXYMECH, the net reaction rate of R2564 reaches

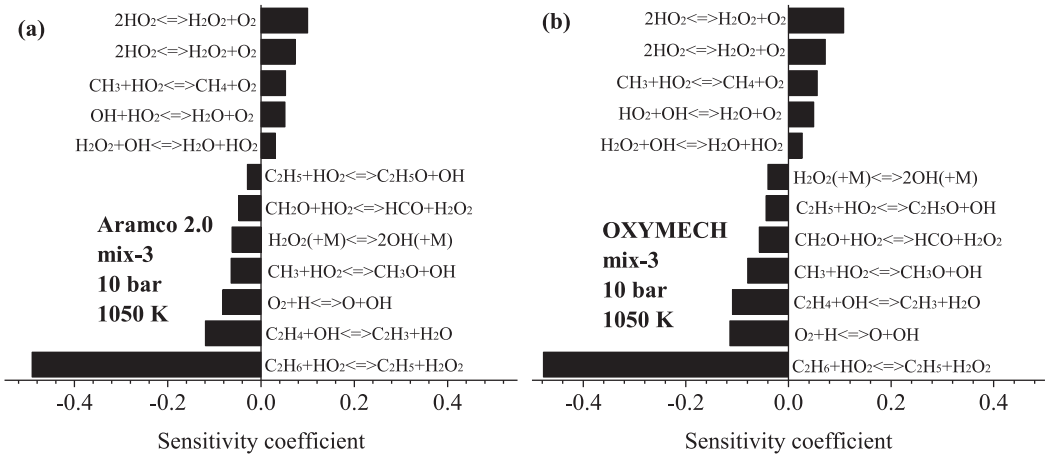

Fig. 6. Sensitivity analysis for mix-3 at $P = 10$ bar and $T = 1050$ K using (a) Aramco 2.0 and (b) OXYMECH.

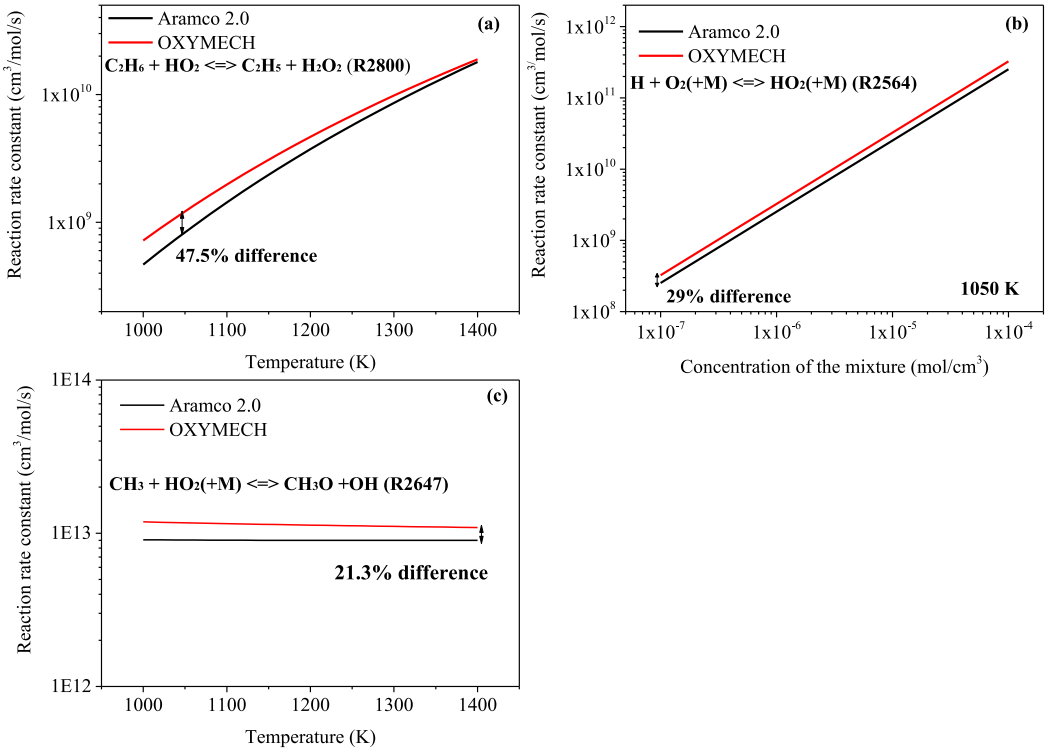

Fig. 7. Comparison of the rate constants obtained from Aramco 2.0 and OXYMECH models for the reactions: (a) $C_2H_6 + HO_2 \Leftrightarrow C_2H_5 + H_2O_2$ (R2800), (b) $H + O_2$ (+M) $\Leftrightarrow$ HO_2 (+M) (R2564), and (c) $CH_3 + HO_2 \Leftrightarrow CH_3O + OH$ (R2647).

a peak value faster, as shown in Fig. 8(c). Moreover, reaction $CH_3 + HO_2 \Leftrightarrow CH_3O + OH$ (R2647) is the most important reactions for HO_2 consumption. As shown in Fig. 7(c), a ~21.3% difference in the rate constant of R2647 between in OXYMECH and Aramco 2.0 is observed [46,67]. As a result, it can be seen from Fig. 8(d) that the net reaction rate of R2647 reaches a peak value faster in OXYMECH than in Aramco 2.0. Therefore, the mole fraction of HO_2 accumulates to high concentrations faster in OXYMECH than in Aramco 2.0, as shown in Fig. 8(e).

H_2O_2 produced through R2800 decomposes into OH rapidly through $H_2O_2 \Leftrightarrow OH + OH$, which is the most important reaction for OH production. R2647 is also the fourth most important reaction for OH production. Therefore, the mole fraction of OH in the OXYMECH calculations reaches a peak value faster than that in the Aramco 2.0 calculations as shown in Fig. 8(f). Thus, the ignition delay times calculated by OXYMECH are significantly shorter than those calculated by Aramco 2.0, in good agreement with the experimental results.

4.5. Comparison of Aramco 2.0 with OXYMECH at P = 10 bar and T = 1350 K

Figure 9 displays the reactions with sensitivity coefficients in the top 12 for mix-3 at $P = 10$ bar and $T = 1350$ K for Aramco 2.0 and OXYMECH. As shown in Fig. 9, the sensitivity coefficient of the reaction $C_2H_4 + H$ (+M) $\Leftrightarrow$ C_2H_5 (+M) (R2773) is negative and in the third place for the two models, which means that R2773 is beneficial for ignition. The rate constant of R2773 in the two models was derived from the calculation results of Miller and Klippenstein [42], but the high-pressure and low-pressure limits were multiplied by a factor of 0.7 in Aramco 2.0, while only the high-pressure limit was multiplied by a factor of 0.9 in OXYMECH. As

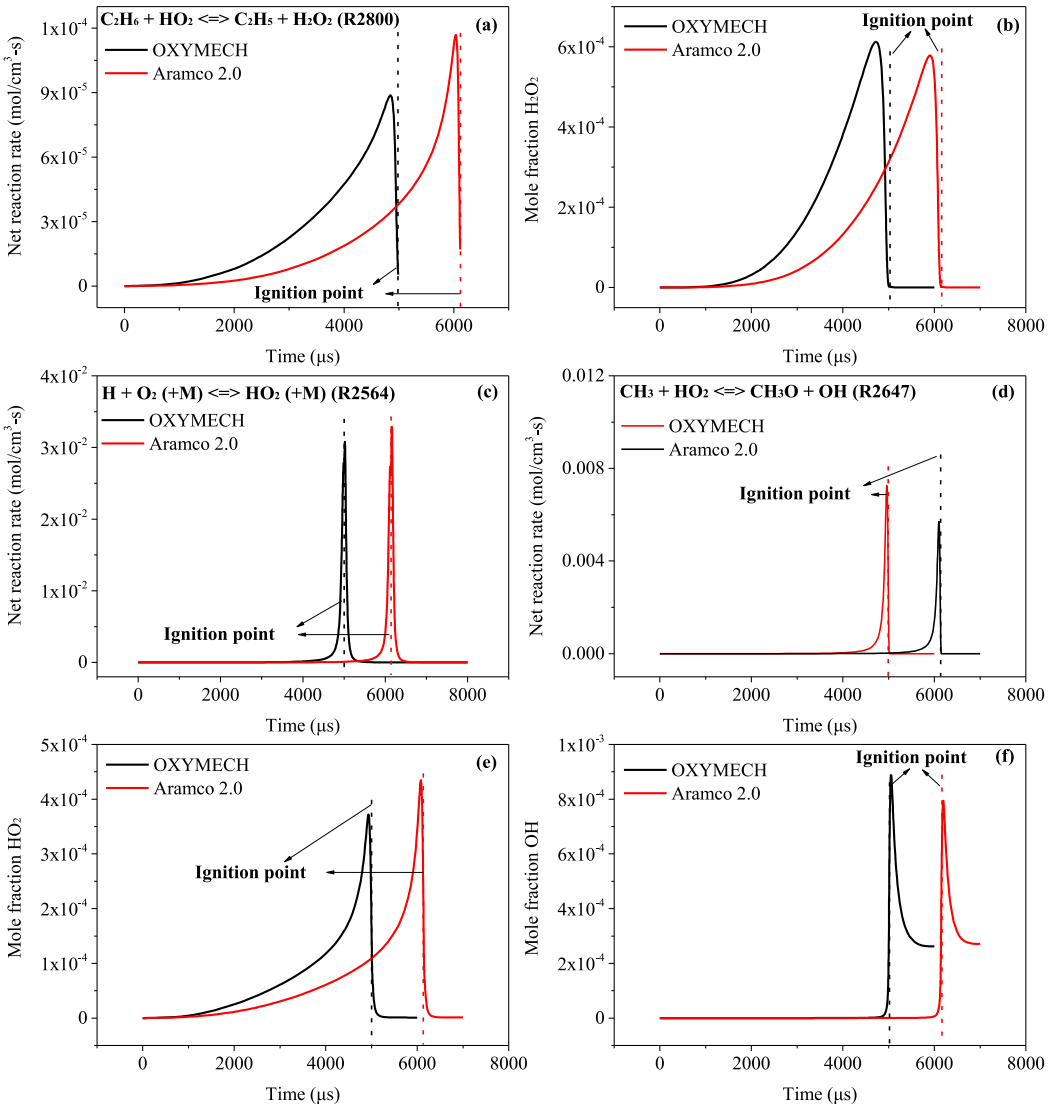

Fig. 8. Comparison of Aramco 2.0 and OXYMECH results at $P = 10$ bar and $T = 1050$ K for the (a) net reaction rate of $C_2H_6 + HO_2 \Leftrightarrow C_2H_5 + H_2O_2$ (R2800), (b) mole fraction of H_2O_2, (c) net reaction rate of $H + O_2(+M) \Leftrightarrow HO_2$ (+M) (R2564), (d) net reaction rate of $CH_3 + HO_2 \Leftrightarrow CH_3O + OH$ (R2647), (e) mole fraction of HO_2, and (f) mole fraction of OH.

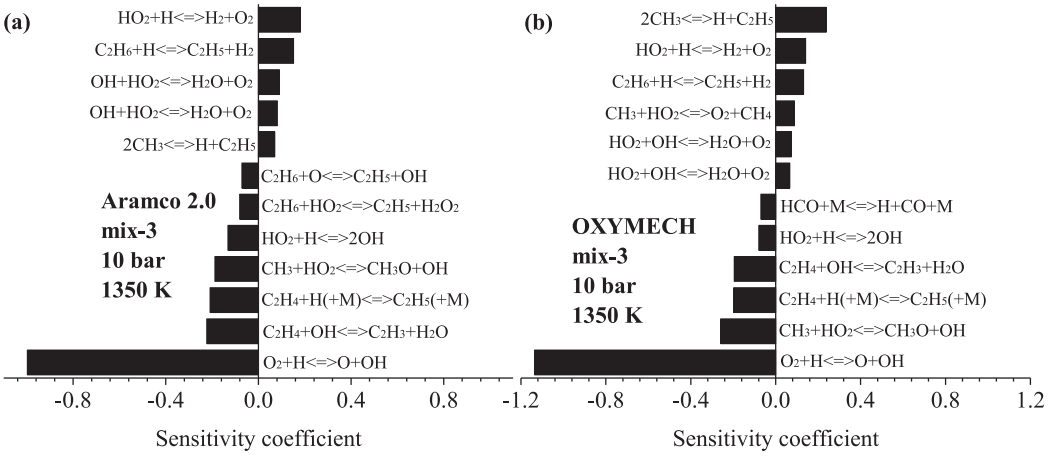

Fig. 9. Sensitivity analysis for mix-3 at $P = 10$ bar and $T = 1350$ K using (a) Aramco 2.0 and (b) OXYMECH.

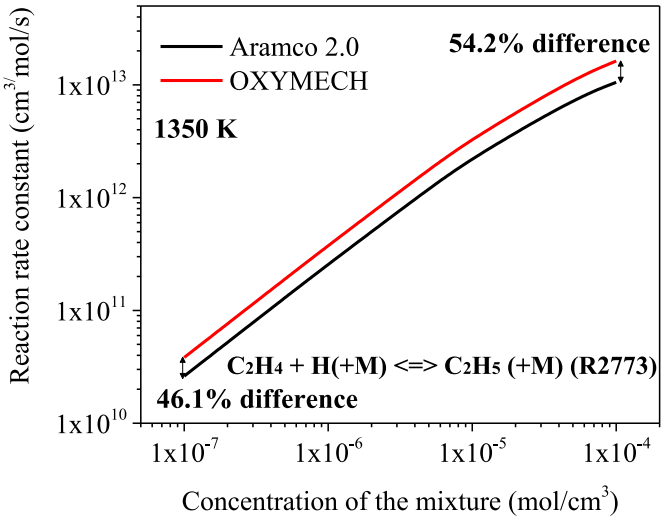

Fig. 10. Comparison of the rate constants from Aramco 2.0 and OXYMECH for the reaction $C_2H_4 + H\ (+M) \Leftrightarrow C_2H_5\ (+M)$ (R2773).

shown in Fig. 10, the differences in the rate constants between OXYMECH and Aramco 2.0 lie between 46.1% and 54.2%. As shown in Fig. 11(a), the net reaction of R2773 for OXYMECH increases faster than that for Aramco 2.0, with a higher peak value. Consequently, OXYMECH provides a higher mole fraction of H that reaches the peak value faster, as shown in Fig. 11(b).

The radical pool reaction $H + O_2 \Leftrightarrow O + OH$ (R2550) has the highest negative sensitivity coefficient. The rate constant of R2550 in the two models was taken from Hong et al. [51], but was multiplied by a factor of 0.95 in OXYMECH according to the recommendation by Smith et al. [27], which is based on a global optimization utilizing a large volume of available experimental data. As a result, the net reaction rate of R2550 in OXYMECH is higher than that in Aramco 2.0, as shown in Fig. 11(c). Furthermore, at 1350 K, the increase in the net reaction rate of R2647 in OXYMECH is still faster than that in Aramco 2.0, fast approaching its peak value, as shown in Fig. 11(d). Because R2647 and R2550 are important reactions for the production of OH, the mole fraction of OH in the OXYMECH calculations reaches a peak value faster than that in the Aramco 2.0 calculations, as shown in Fig. 11(e).

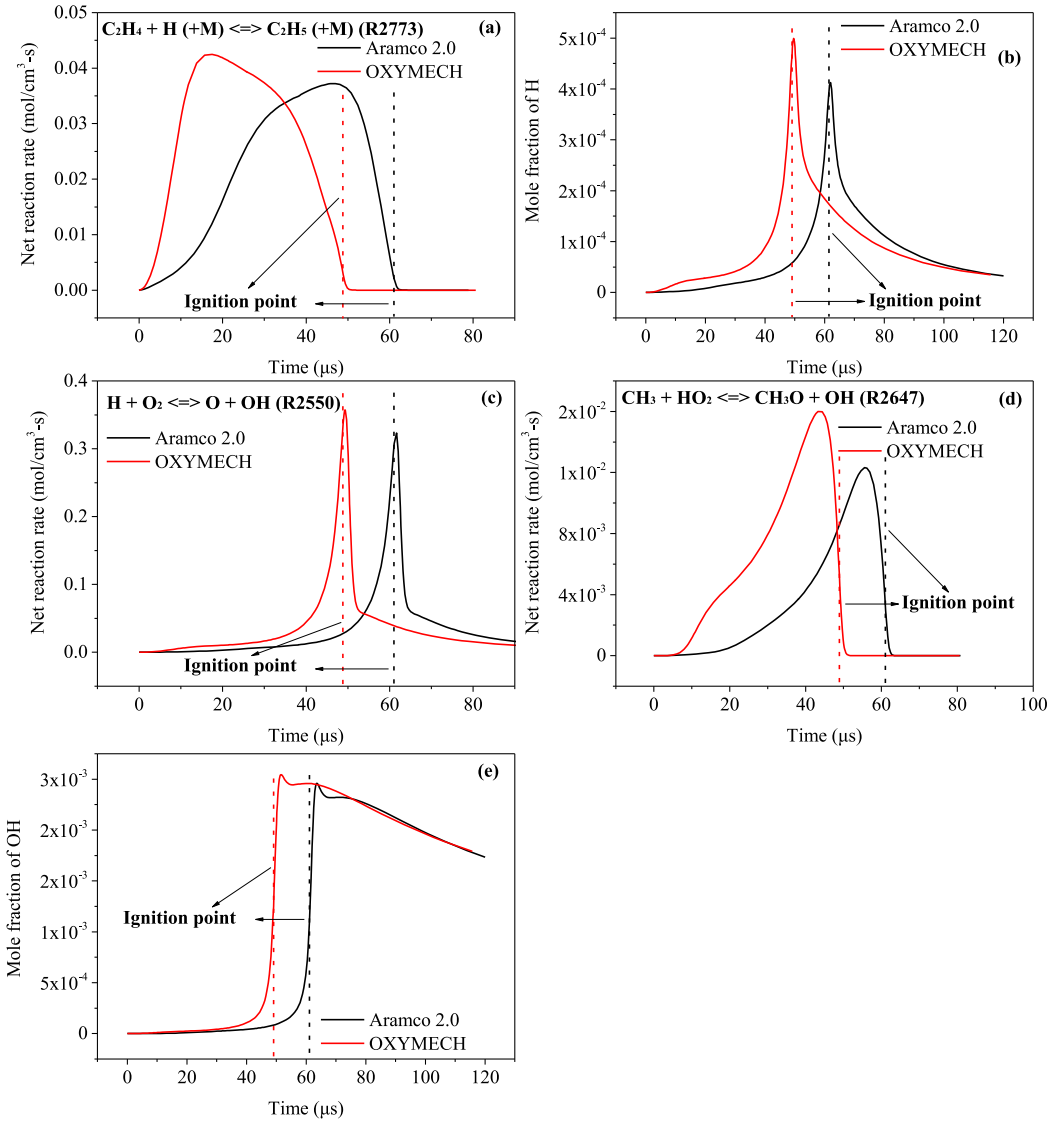

Fig. 11. Comparison of Aramco 2.0 and OXYMECH results at $P = 10$ bar and $T = 1350$ K for the (a) net reaction rate $C_2H_4 + H\ (+M) \Leftrightarrow C_2H_5\ (+M)$ (R2773), (b) mole fraction of H, (c) net reaction rate of $H + O_2 \Leftrightarrow O + OH$ (R2550), (d) net reaction rate of $CH_3 + HO_2 \Leftrightarrow CH_3O + OH$ (R2647), and (e) mole fraction of OH.

5. Conclusion

The ignition delay times of ethane under O_2/CO_2 atmosphere were measured in a shock tube. The experimental results suggest that the ignition delay times decrease with the increasing ethane concentration at 0.8, 2.0, and 10 bar, while the effect of the fuel concentration on the ignition delay times of ethane under O_2/CO_2 atmosphere is not sensitive to the pressure. The ignition delay times of ethane under O_2/CO_2 atmosphere increases with the increasing equivalence ratio at 0.8 and 2.0 bar, while the effect of the equivalence ratio decreases with the increasing pressure from 0.8 to 2.0 bar. At 10 bar, the effect of the equivalence ratio on the ignition delay times of ethane further weaken at high temperatures, while the ignition delay times decrease with the increasing equivalence ratio in the low temperature range. High concentrations of CO_2 significantly increase the ignition delay times of ethane at 10 bar, while its effect is minimal at 0.8 and 2.0 bar.

A reaction model for pressurized oxy-fuel combustion, named OXYMECH, was developed and updated based on our previous work. Three detailed chemical models (Aramco 2.0, "Ranzi", and OXYMECH) were evaluated using the present experimental data. Detailed comparisons revealed that the OXYMECH predictions are in good agreement with the experimental data, while Aramco 2.0 affords significant overprediction of the experimental results at $P = 10$ bar.

At 10 bar, underestimation of the reaction rates of $C_2H_6 + HO_2 \Leftrightarrow C_2H_5 + H_2O_2$, $H + O_2\ (+M) \Leftrightarrow HO_2\ (+M)$, $CH_3 + HO_2 \Leftrightarrow CH_3O + OH$, and $2HO_2 \Leftrightarrow H_2O_2 + O_2$ results in overprediction of Aramco 2.0 in the low temperature region. Moreover, underestimation of the reaction rates of $C_2H_4 + H\ (+M) \Leftrightarrow C_2H_5\ (+M)$ and $H + O_2 \Leftrightarrow O + OH$ is the reason for the overprediction of Aramco 2.0 at high temperatures. Updating the rate constants of these six reactions contributes to the superior performance of the OXYMECH model.

Acknowledgments

The authors thank for Professor Jyh-YuanChen form Department of Mechanical Engineering, University of California – Berkeley for his help in performing sensitivity analysis. This work was supported by the general program (No. 51776081) of the National Natural Science Foundation of China.

Supplementary material

Supplementary material associated with this article can be found, in the online version, at doi:10.1016/j.combustflame.2019.03.031.

References

[1] L. Chen, S.Z. Yong, A.F. Ghoniem, Oxy-fuel combustion of pulverized coal: characterization, fundamentals, stabilization and CFD modeling, Prog. Energy Combust. Sci. 38 (2012) 156–214.
[2] J. Hong, R. Field, M. Gazzino, A.F. Ghoniem, Operating pressure dependence of the pressurized oxy-fuel combustion power cycle, Energy 35 (2010) 5391–5399.
[3] H. Zebian, A. Mitsos, Pressurized oxy-coal combustion: ideally flexible to uncertainties, Energy 57 (2013) 513–526.
[4] F. Xia, Z. Yang, A. Adeosun, A. Gopan, B.M. Kumfer, R.L. Axelbaum, Pressurized oxy-combustion with low flue gas recycle: computational fluid dynamic simulations of radiant boilers, Fuel 181 (2016) 1170–1178.
[5] S. Barak, O. Pryor, J. Lopez, E. Ninnemann, S. Vasu, B. Koroglu, High-speed imaging and measurements of ignition delay times in oxy-syngas mixtures with high CO_2 dilution in a shock tube with high-speed imaging, J. Eng. Gas Turbines Power 137 (2017) 121503–121507.
[6] J. Shao, R. Choudhary, D.F. Davidson, R.K. Hanson, S. Barak, S. Vasu, Ignition delay times of methane and hydrogen highly diluted in carbon dioxide at high pressures up to 300 atm, Proc. Combust. Inst. 37 (2018) 4555–4562.
[7] O. Pryor, S. Barak, J. Lopez, E. Ninnemann, B. Koroglu, L. Nash, S. Vasu, High pressure shock tube ignition delay time measurements during oxy-methane combustion with high levels of CO_2 dilution, J. Energy Resour. Technol. 139 (2017) 0422081–0422086.
[8] S.S. Vasu, D.F. Davidson, R.K. Hanson, Shock tube study of syngas ignition in rich CO_2 mixtures and determination of the rate of $H + O_2 + CO_2 \rightarrow HO_2 + CO_2$, Energy Fuels 25 (2011) 990–997.
[9] B. Koroglu, O.M. Pryor, J. Lopez, L. Nash, S.S. Vasu, Shock tube ignition delay times and methane time-histories measurements during excess CO_2 diluted oxy-methane combustion, Combust. Flame 164 (2016) 152–163.
[10] J.W. Hargis, E.L. Petersen, Methane ignition in a shock tube with high levels of CO_2 dilution: consideration of the reflected-shock bifurcation, Energy Fuels 29 (2015) 7712–7726.
[11] H. Hashemi, J.G. Jacobsen, C.T. Rasmussen, J.M. Christensen, P. Glarborg, S. Gersen, M. van Essen, H.B. Levinsky, S.J. Klippenstein, High-pressure oxidation of ethane, Combust. Flame 182 (2017) 150–166.
[12] P. Dagaut, M. Cathonnet, J.c. Boettner, Kinetics of ethane oxidation, Int. J. Chem. Kinet. 23 (1991) 437–455.
[13] M.S. Shokrollahi Yancheshmeh, S. Seifzadeh Haghighi, M.R. Gholipour, O. Dehghani, M.R. Rahimpour, S. Raeissi, Modeling of ethane pyrolysis process: a study on effects of steam and carbon dioxide on ethylene and hydrogen productions, Chem. Eng. J. 215–216 (2013) 550–560.
[14] S. Wang, Q. Feng, F. Javadpour, Q. Hu, K. Wu, Competitive adsorption of methane and ethane in montmorillonite nanopores of shale at supercritical conditions: a grand canonical Monte Carlo simulation study, Chem. Eng. J. 355 (2019) 76–90.
[15] L. Pan, Y. Zhang, J. Zhang, Z. Tian, Z. Huang, Shock tube and kinetic study of $C_2H_6/H_2/O_2$/Ar mixtures at elevated pressures, Int. J. Hydrog. Energy 39 (2014) 6024–6033.
[16] E. Hu, Y. Chen, Z. Zhang, X. Li, Y. Cheng, Z. Huang, Experimental study on ethane ignition delay times and evaluation of chemical kinetic models, Energy Fuels 29 (2015) 4557–4566.
[17] J. Zhang, E. Hu, Z. Zhang, L. Pan, Z. Huang, Comparative study on ignition delay times of C_1–C_4 alkanes, Energy Fuels 27 (2013) 3480–3487.
[18] J. de Vries, J.M. Hall, S.L. Simmons, M.J. Rickard, D.M. Kalitan, E.L Petersen, Ethane ignition and oxidation behind reflected shock waves, Combust. Flame 150 (2007) 137–150.
[19] C.J. Aul, W.K. Metcalfe, S.M. Burke, H.J. Curran, E.L. Petersen, Ignition and kinetic modeling of methane and ethane fuel blends with oxygen: a design of experiments approach, Combust. Flame 160 (2013) 1153–1167.
[20] W.K. Metcalfe, S.M. Burke, S.S. Ahmed, H.J. Curran, A hierarchical and comparative kinetic modeling study of $C_1 - C_2$ hydrocarbon and oxygenated fuels, Int. J. Chem. Kinet. 45 (2013) 638–675.
[21] Smith, G.P.; Golden, D.M.; Frenklach, M.; Moriarty, N.W.; Eiteneer, B.; Goldenberg, M.; Bowman, C.T.; Hanson, R.K.; Song, S.; Gardiner, W.C., Jr. GRI-Mech 3.0, 1999; http://www.me.berkeley.edu/gri_mech/.
[22] D. Healy, D.M. Kalitan, C.J. Aul, E.L. Petersen, G. Bourque, H.J. Curran, Oxidation of C_1–C_5 alkane quinternary natural gas mixtures at high pressures, Energy Fuels 24 (2010) 1521–1528.
[23] H. Wang, X.Q. You, A.V. Joshi, S.G. Davis, A. Laskin, F. Egolfopoulos, C.K. Law, USC mech version II. High-temperature combustion reaction model of $H_2/CO/C_1$-C_4 compounds, University of Southern California, Los Angeles, CA, 2007 http://ignis.usc.edu/USC_Mech_II.htm.
[24] Y. Liu, C. Zou, J. Cheng, H. Jia, C. Zheng, Experimental and numerical study of the effect of CO_2 on the ignition delay times of methane under different pressures and temperatures, Energy Fuels 32 (2018) 10999–11009.
[25] S. Barak, E. Ninnemann, S. Neupane, F. Barnes, J. Kapat, S. Vasu, High-pressure oxy-syngas ignition delay times with CO_2 dilution: shock tube measurements and comparison of the performance of kinetic mechanisms, J. Eng. Gas Turbines Power 141 (2018) 021011–021017.
[26] L. Cai, S. Kruse, D. Felsmann, C. Thies, K.K. Yalamanchi, H. Pitsch, Experimental design for discrimination of chemical kinetic models for oxy-methane combustion, Energy Fuels 31 (2017) 5533–5542.
[27] Smith, G.P.; Tao, Y.; Wang, H. Foundational Fuel Chemistry Model, Version 1.0 (FFCM-1), 2016; http://nanoenergy.stanford.edu/ffcm1.
[28] E. Ranzi, A. Frassoldati, R. Grana, A. Cuoci, T. Faravelli, A.P. Kelley, C.K. Law, Hierarchical and comparative kinetic modeling of laminar flame speeds of hydrocarbon and oxygenated fuels, Prog. Energy Combust. Sci. 38 (2012) 468–501.
[29] Y. Li, C.-W. Zhou, K.P. Somers, K. Zhang, H.J. Curran, The oxidation of 2-butene: a high pressure ignition delay, kinetic modeling study and reactivity comparison with isobutene and 1-butene, Proc. Combust. Inst. 36 (2017) 403–411.
[30] H.C. Lee, A.A. Mohamad, L.Y. Jiang, Comprehensive comparison of chemical kinetics mechanisms for syngas/biogas mixtures, Energy Fuels 29 (2015) 6126–6145.
[31] R.K. Hanson, D.F. Davidson, Recent advances in laser absorption and shock tube methods for studies of combustion chemistry, Prog. Energy Combust. Sci. 44 (2014) 103–114.
[32] J. Shao, R. Choudhary, A. Susa, D.F. Davidson, R.K. Hanson, Shock tube study of the rate constants for $H + O_2 + M \rightarrow HO_2 + M$ ($M = Ar, H_2O, CO_2, N_2$) at elevated pressures, Proc. Combust. Inst. 37 (2018) 145–152.
[33] S. Wang, D.F. Davidson, R.K. Hanson, Shock tube and laser absorption study of CH_2O oxidation via simultaneous measurements of OH and CO, J. Phys. Chem. A 121 (2017) 8561–8568.
[34] Morley, C. Gaseq, Version 0.76; http://www.gaseq.co.uk.
[35] E.L. Petersen, R.K. Hanson, Measurement of reflected-shock bifurcation over a wide range of gas composition and pressure, Shock Waves 15 (2006) 333–340.

[36] D.A. Sheen, X. You, H. Wang, T. Løvås, Spectral uncertainty quantification, propagation and optimization of a detailed kinetic model for ethylene combustion, Proc. Combust. Inst. 32 (2009) 535–542.
[37] D.A. Sheen, H. Wang, Combustion kinetic modeling using multispecies time histories in shock-tube oxidation of heptane, Combust. Flame 158 (2011) 645–656.
[38] Y. Tao, G.P. Smith, H. Wang, Critical kinetic uncertainties in modeling hydrogen/carbon monoxide, methane, methanol, formaldehyde, and ethylene combustion, Combust. Flame 195 (2018) 18–29.
[39] D.L. Baulch, C.T. Bowman, C.J. Cobos, R.A. Cox, T. Just, J.A. Kerr, M.J. Pilling, D. Stocker, J. Troe, W. Tsang, R.W. Walker, J. Warnatz, Evaluated kinetic data for combustion modeling: supplement II, J. Phys. Chem. Ref. Data 34 (2005) 757–1397.
[40] N. Cohen, The use of transition-state theory to extrapolate rate coefficients for reactions of H atoms with alkanes, Int. J. Chem. Kinet. 23 (1991) 683–700.
[41] J.A. Miller, S.J. Klippenstein, The reaction between ethyl and molecular oxygen II: further analysis, Int. J. Chem. Kinet. 33 (2001) 654–668.
[42] J.A. Miller, S.J. Klippenstein, The $H + C_2H_2$ (+ M) $\rightleftarrows$ C_2H_3 (+M) and $H + C_2H_2$ (+M) $\rightleftarrows$ C_2H_5 (+M) reactions: electronic structure, variational transition-state theory, and solutions to a two-dimensional master equation, Phys. Chem. Chem. Phys. 6 (2004) 1192–1202.
[43] S.S. Vasu, Z. Hong, D.F. Davidson, R.K. Hanson, D.M. Golden, Shock tube/laser absorption measurements of the reaction rates of OH with ethylene and propene, J. Phys. Chem. A 114 (2010) 11529–11537.
[44] P.H. Stewart, C.W. Larson, D.M. Golden, Pressure and temperature dependence of reactions proceeding via a bound complex. 2. Application to $2CH_3 \rightarrow C_2H_5 + H$, Combust. Flame 75 (1989) 25–31.
[45] J.J. Scire, R.A. Yetter, F.L. Dryer, Flow reactor studies of methyl radical oxidation reactions in methane-perturbed moist carbon monoxide oxidation at high pressure with model sensitivity analysis, Int. J. Chem. Kinet. 33 (2001) 75–100.
[46] R. Zhu, C. Lin, The $CH_3 + HO_2$ reaction: first-principles prediction of its rate constant and product branching probabilities, J. Phys. Chem. A 105 (2001) 6243–6248.
[47] A.W. Jasper, S.J. Klippenstein, L.B. Harding, Theoretical rate coefficients for the reaction of methyl radical with hydroperoxyl radical and for methylhydroperoxide decomposition, Proc. Combust. Inst. 32 (2009) 279–286.
[48] N.K. Srinivasan, J.V. Michael, L.B. Harding, S.J. Klippenstein, Experimental and theoretical rate constants for $CH_4 + O_2 \rightarrow CH_3 + HO_2$, Combust. Flame 149 (2007) 104–111.
[49] A.V. Joshi, H. Wang, Master equation modeling of wide range temperature and pressure dependence of $CO + OH \rightarrow$ products, Int. J. Chem. Kinet. 38 (2006) 57–73.
[50] J. Troe, The thermal dissociation/recombination reaction of hydrogen peroxide H2O2 (+M) ⇔ 2OH (+M) III.: analysis and representation of the temperature and pressure dependence over wide ranges, Combust. Flame 158 (2011) 594–601.
[51] Z. Hong, D.F. Davidson, E.A. Barbour, R.K. Hanson, A new shock tube study of the $H + O_2 \rightarrow OH + O$ reaction rate using tunable diode laser absorption of H_2O near 2.5 μm, Proc. Combust. Inst. 33 (2011) 309–316.
[52] C. Kappel, K. Luther, J. Troe, Shock wave study of the unimolecular dissociation of H_2O_2 in its falloff range and of its secondary reactions, Phys. Chem. Chem. Phys. 4 (2002) 4392–4398.
[53] J.V. Michael, J.W. Sutherland, L.B. Harding, A.F. Wagner, Initiation in H_2/O_2: rate constants for $H_2 + O_2 \rightarrow H + HO_2$ at high temperature, Proc. Combust. Inst. 28 (2000) 1471–1478.
[54] M. Mueller, T. Kim, R. Yetter, F. Dryer, Flow reactor studies and kinetic modeling of the H_2/O_2 reaction, Int. J. Chem. Kinet. 31 (1999) 113–125.
[55] J. Michael, J. Sutherland, Rate constant for the reaction of H with H/sub 2/O and OH with H/sub 2/by the flash photolysis-shock tube technique over the temperature range 1246–2297 K, J. Phys. Chem. 92 (1988) 92.
[56] J. Troe, Detailed modeling of the temperature and pressure dependence of the reaction H+ O_2 (+ M)→ HO_2 (+ M), Proc. Combust. Inst. 28 (2000) 1463–1469.
[57] AE Lutz, RJ Kee, JA Miller, SENKIN: A FORTRAN program for predicting homogeneous gas phase chemical kinetics with sensitivity analysis, Sandia National Labs, Livermore, CAUSA, 1988.
[58] Reaction Design, CHEMKIN-PRO 15083, Reaction Design, San Diego, CA, 2008.
[59] P. Sabia, M. Lubrano Lavadera, P. Giudicianni, G. Sorrentino, R. Ragucci, M. de Joannon, CO_2 and H_2O effect on propane auto-ignition delay times under mild combustion operative conditions, Combust. Flame 162 (2015) 533–543.
[60] D.J. Seery, C.T. Bowman, An experimental and analytical study of methane oxidation behind shock waves, Combust. Flame 14 (1970) 37–47.
[61] E.L. Petersen, D.F. Davidson, R.K. Hanson, Ignition delay times of ram accelerator CH/O/diluent mixtures, J. Propuls. Power 15 (1999) 82–91.
[62] Y. Zhang, Z. Huang, L. Wei, J. Zhang, C.K. Law, Experimental and modeling study on ignition delays of lean mixtures of methane, hydrogen, oxygen, and argon at elevated pressures, Combust. Flame 159 (2012) 918–931.
[63] G.A. Pang, D.F. Davidson, R.K. Hanson, Experimental study and modeling of shock tube ignition delay times for hydrogen–oxygen–argon mixtures at low temperatures, Proc. Combust. Inst. 32 (2009) 181–188.
[64] A. Kéromnès, W.K. Metcalfe, K.A. Heufer, N. Donohoe, A.K. Das, C.-J. Sung, J. Herzler, C. Naumann, P. Griebel, O. Mathieu, M.C. Krejci, E.L. Petersen, W.J. Pitz, H.J. Curran, An experimental and detailed chemical kinetic modeling study of hydrogen and syngas mixture oxidation at elevated pressures, Combust. Flame 160 (2013) 995–1011.
[65] J. Aguilera-Iparraguirre, H.J. Curran, W. Klopper, J.M. Simmie, Accurate benchmark calculation of the reaction barrier height for hydrogen abstraction by the hydroperoxyl radical from methane. Implications for C_nH_{2n+2} where $n = 2 \rightarrow 4$, J. Phys. Chem. A 112 (2008) 7047–7054.
[66] R. Fernandes, K. Luther, J. Troe, V. Ushakov, Experimental and modelling study of the recombination reaction H+ O_2 (+ M)→ HO_2 (+ M) between 300 and 900 K, 1.5 and 950 bar, and in the bath gases M = He, Ar, and N_2, Phys. Chem. Chem. Phys. 10 (2008) 4313–4321.
[67] A.W. Jasper, S.J. Klippenstein, L.B. Harding, Theoretical rate coefficients for the reaction of methyl radical with hydroperoxyl radical and for methylhydroperoxide decomposition, Proc. Combust. Inst. 32 (2009) 279–286.